Conformal Scalar Field Theory from Ising Tricriticality on the Fuzzy Sphere

Joseph Taylor,[1] Cristian Voinea,[1] Zlatko Papić,[1] and Ruihua Fan[2]
[1]School of Physics and Astronomy, University of Leeds, Leeds LS2 9JT, United Kingdom
[2]Department of Physics, University of California, Berkeley, California 94720, USA

(Received 7 July 2025; accepted 24 December 2025; published 6 February 2026)

Free theories are landmarks in the landscape of quantum field theories: their exact solvability serves as a pillar for perturbative constructions of interacting theories. Fuzzy sphere regularization, which combines quantum Hall physics with state-operator correspondence, has recently been proposed as a promising framework for simulating three-dimensional conformal field theories (CFTs), but so far it has not provided access to free theories. We overcome this limitation by designing a bilayer quantum Hall system that hosts an Ising tricritical point—a nontrivial fixed point where first-order and second-order transitions meet—which flows to the conformally coupled scalar theory in the infrared. The critical energy spectrum and operator structure match those at the Gaussian fixed point, providing nonperturbative evidence for the emergence of a free scalar CFT. Our results expand the landscape of CFTs realizable on the fuzzy sphere and demonstrate that even free bosonic theories—previously inaccessible—can emerge from interacting electrons in this framework.

DOI: 10.1103/cj3l-cf58

Introduction—Understanding quantum field theories (QFTs) in dimensions higher than two remains a central challenge in theoretical physics, especially in the conformally invariant regime where perturbative methods often fail [1–3]. The fuzzy sphere regularization, which combines state-operator correspondence [4] with insights from quantum Hall physics [5], has recently emerged as a powerful framework for simulating three-dimensional (3D) conformal field theories (CFTs) [6]. This approach enables the computation of operator-product expansion coefficients and correlators [7,8], conformal generators [9,10], entropic F functions [11], and study of defects and surface CFTs [12–15]. It has successfully captured a range of interacting theories, including the 3D Ising and $O(N)$ Wilson-Fisher models [6,16–18], deconfined quantum critical points [19–22], the pseudocritical Potts model [23], nonunitary Yang-Lee models [24–26], and other new classes of CFTs [27].

One glaring exception in the set of theories realized on the fuzzy sphere are *free* CFTs. As exactly solvable models, free CFTs are reference points for elucidating the fundamental structural features of QFTs and analyzing strongly interacting systems. Therefore, they not only play a foundational role in QFT as well as many-body physics more broadly. The realization of free theories on the fuzzy sphere would not only be a step toward establishing the completeness of the fuzzy sphere regularization but would also offer conceptual insights into its mechanism.

In this Letter, we show how to realize the simplest free CFT—the conformally coupled scalar, which we refer to as the free scalar throughout this Letter. At first glance, it may seem unlikely that a free bosonic theory could emerge from a system of strongly interacting electrons in the lowest Landau level (LLL), which the fuzzy sphere method utilizes. The key insight comes from the nature of Ising tricriticality, described by the Euclidean Lagrangian, $\mathcal{L}_E = (\partial\phi)^2 + g\phi^6$, in flat space. In 3D, the ϕ^6 interaction is marginally irrelevant at the Gaussian fixed point, so a system at tricriticality will flow toward the free scalar CFT in the deep infrared (IR) [28,29]. This perspective provides a natural route to the free scalar: tune a quantum Hall Ising ferromagnetic transition to its tricritical point.

Specifically, we design a bilayer quantum Hall system that realizes both an Ising transition line and a first-order transition line, and most importantly, Ising tricriticality at their intersection point. Our two-component model is conceptually different from the standard one of tricriticality based on spin-1 degrees of freedom [30,31]. With appropriate fine-tuning, our model at the tricritical point is characterized by a free scalar CFT up to small residual interactions, which we demonstrate by the matching of the low-energy spectra and the emergence of the characteristic free-boson algebra.

The model—Consider a quantum Hall bilayer on a sphere [32]. Setting the filling factor and magnetic length to unity, the number of flux quanta N_ϕ, the number of electrons N, and the radius R are related by $N_\phi = N - 1 = 2R^2$.

Let $c_{a=\uparrow,\downarrow}(\boldsymbol{r})$ denote the LLL-projected electron annihilation operators for the two pseudospin species in real space. The Hamiltonian reads

$$H = H_{\text{inter}} + \lambda H_{\text{intra}} - h\int \left(c_\uparrow^\dagger(\boldsymbol{r})c_\downarrow(\boldsymbol{r}) + \text{H.c.}\right)d^2\boldsymbol{r},$$
$$H_{\text{inter}} = 2\int V(\boldsymbol{r}_1-\boldsymbol{r}_2)n_\uparrow(\boldsymbol{r}_1)n_\downarrow(\boldsymbol{r}_2)d^2\boldsymbol{r}_1 d^2\boldsymbol{r}_2,$$
$$H_{\text{intra}} = \sum_{a=\uparrow,\downarrow}\int U(\boldsymbol{r}_1-\boldsymbol{r}_2):n_a(\boldsymbol{r}_1)n_a(\boldsymbol{r}_2):d^2\boldsymbol{r}_1 d^2\boldsymbol{r}_2, \quad (1)$$

where $n_a(\boldsymbol{r}) = c_a^\dagger(\boldsymbol{r})c_a(\boldsymbol{r})$ and $::$ denotes normal ordering. The intralayer and interlayer interactions, U and V, to be specified below, are assumed to be predominantly repulsive and we parametrize them by the Haldane pseudopotentials, U_J and V_J [32]. We keep charge degrees of freedom gapped and let the pseudospins undergo a transition.

Compared to the 3D Ising fuzzy sphere model [6], our Hamiltonian (1) contains an extra intralayer interaction term, which plays a crucial role in realizing the first-order transition. This can be understood at the mean-field level via a Hartree-Fock approximation. As shown in Supplemental Material (SM) [33], the phase boundary is given by $h = 2(1-\lambda)\sum_J(V_{2J+1} - U_{2J+1})$. Fixing V and U, the system is ferromagnetic at small values of λ and h, and paramagnetic otherwise. The transition is second order for all $h > 0$ and becomes first order only at $h = 0$. Although the mean-field analysis does not capture the tricritical point on the phase boundary, it highlights the necessity of including intralayer interactions to realize first-order behavior. Below, we will see that fluctuations beyond mean field qualitatively modify the critical behavior near $h = 0$, giving rise to richer phase structures that *do* contain a tricritical point.

Phase diagram and tricritical point—Unlike in two dimensions, where imposing the Kramers-Wannier duality reduces the number of $\mathbb{Z}_2$-even relevant perturbations from two to one, no such counterpart exists in 3D [34–36]. As a result, reaching the tricritical point requires careful tuning of parameters. Moreover, because the equivalence to the free scalar theory emerges only asymptotically in the IR, additional fine tuning is necessary to suppress finite-size effects, particularly those stemming from the marginal ϕ^6 and irrelevant operators.

In our case, we first fix $\lambda = 1$ and use gradient descent in the residual parameter space to identify a point whose energy spectrum closely matches that of the free scalar. We then perform two consistency checks: (1) vary λ and h to map out the full phase diagram and confirm that the identified point is at a tricritical juncture, and (2) explicitly demonstrate that the spectrum at this point is well approximated by a free scalar CFT, even in system sizes beyond those for which the optimization was performed.

We use gradient descent optimization over five parameters: two intralayer pseudopotentials (U_3, U_5), two interlayer ones (V_0, V_2), and the transverse field h. As a consequence of fermionic exchange statistics, we can fix $U_0 = U_2 = U_4 = 0$; moreover, we fix $U_1 = V_1 = 1$ to avoid overfitting and accidental symmetries [33]. Importantly, we also impose an additional constraint to avoid spurious local minima, where the spectrum seems conformal but the ground state wave function is actually gapped [33]. Performing the described optimization for $N = 10$, we arrive at $\{U_1, U_3, U_5\} \approx \{1, 0.07, -0.13\}$, $\{V_0, V_1, V_2\} \approx \{2.35, 1, 0.37\}$, $h \approx 0.23$. We emphasize that these parameter values will be used for all system sizes considered below. Note that the short range and negative pseudopotentials make this interaction quite different from the standard quantum Hall bilayers [37]. With these parameters, the low-energy spectra for different system sizes match the free scalar theory, as we discuss in detail below, and the energy gap vanishes as $1/\sqrt{N}$ [33].

Fixing the optimized parameters, we vary the overall intralayer interaction strength λ and transverse field h to map out the two-dimensional phase diagram shown in Fig. 1(a). At large h, mean-field analysis predicts a second-order transition, which is expected to fall into the Ising

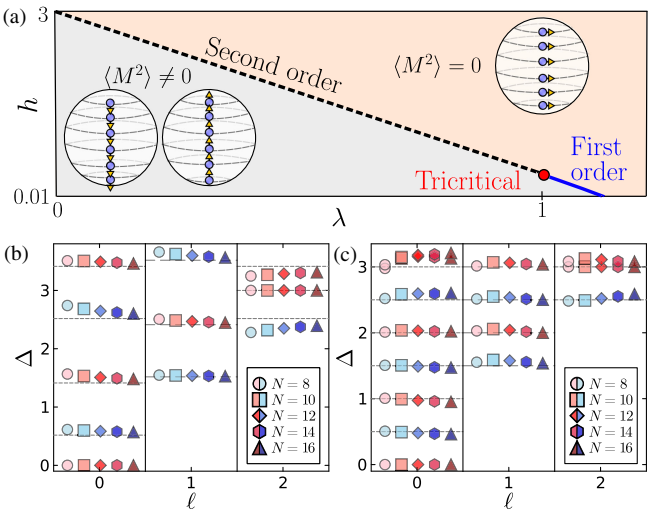

FIG. 1. Phase diagram and representative energy spectra. (a) The line of 3D Ising transitions (black dashed line) meets the line of first-order transitions (blue line) at a tricritical point $(\lambda, h) \approx (1.0, 0.23)$ (red dot). The shaded regions correspond to ordered and disordered phases according to the value of the magnetization $\langle M^2\rangle$. (b) The energy spectrum as a function of angular momentum ℓ at a representative point $(\lambda, h) = (0.4, 2)$ along the 3D Ising line. Data are for several system sizes shown in the legend, while red and blue symbols indicate $\mathbb{Z}_2$-even and odd states, respectively. We rescale the spectrum so that the first spin-2, $\mathbb{Z}_2$-even state lies at energy 3. (c) Same as (b) but taken at the tricritical point. While the spectrum in (b) shows good agreement with 3D Ising CFT [6], the spectrum in (c) is consistent with free scalar theory, with (half-) integral energies alternating in $\mathbb{Z}_2$ parity.

universality class upon including fluctuations. Here, we estimate the location of the Ising critical line by leveraging state-operator correspondence. Specifically, we define a cost function that compares the low-energy spectrum at each (λ, h) to that of the 3D Ising CFT. At a fixed system size $N = 12$, we find the cost function exhibits a minimum along a line in parameter space [33], which defines the black dashed line in Fig. 1(a). Following this line toward smaller h, we find the ground state energy density as a function of λ starts to develop a kink, suggesting that a continuous phase transition gives way to a first-order line [blue line in Fig. 1(a)], with the optimized parameter sitting in between as the putative tricritical point [red dot in Fig. 1(a)].

Before presenting the supporting numerical analysis of the phase diagram, we point out one subtlety at $h = 0$. In this regime, the particle number of each pseudospin component is conserved and increasing λ leads to a first-order transition at $\lambda \gtrsim 1$, from one of the layers being fully filled, $\nu_\uparrow = 1$, $\nu_\downarrow = 0$ (or vice versa) to $(\nu_\uparrow, \nu_\downarrow) = (1/2, 1/2)$ [33]. While this occurs as a level crossing, consistent with our Fig. 1(a), the state $(\nu_\uparrow, \nu_\downarrow) = (1/2, 1/2)$ describes two charge-gapless composite fermion Fermi seas rather than a gapped paramagnet [38]. To avoid this, our phase diagram in Fig. 1(a) starts from a small but nonzero value of $h = 0.01$, which is sufficient to open up a gap near $\lambda = 1$ [33].

Along the dashed black line in Fig. 1(a), the low-energy spectrum closely matches that of the 3D Ising CFT [6]. Figure 1(b) shows the spectrum at a representative point $(\lambda, h) = (0.40, 2.0)$, whose location is refined via finite-size scaling beyond the system size for the optimization.

By contrast, the energy spectrum at the optimized parameter values closely matches that of the free scalar CFT, as shown in Fig. 1(c). It is easiest to verify this matching via the state-operator correspondence. Recall the Euclidean Lagrangian of the free scalar $\mathcal{L}_E = (\partial\phi)^2/2$ in $\mathbb{R}^3$. The field ϕ is a scalar primary with the scaling dimension $\Delta = 1/2$. All other local operators are built from powers of ϕ and its derivatives, such as ϕ^n, $\partial_\mu \phi^n$, etc., which thus have integral or half-integral scaling dimensions [33]. This is indeed consistent with Fig. 1(c). A more detailed inspection reveals additional fingerprints of the free scalar theory. For example, since ϕ satisfies the equation of motion $\Box\phi = 0$, the level-2 scalar descendant $\Box\phi$ vanishes. Consequently, we expect only a single state at $\Delta = 5/2$—precisely as observed in the numerical result. In contrast, for composite operators like ϕ^2, $\Box\phi^2 \neq 0$, and we indeed observe two scalar states near $\Delta = 3$, with the other being the primary ϕ^6. Similarly, two spin-2 states appear at $\Delta = 3$, corresponding to the stress-energy tensor and the spin-2 descendant of ϕ^2, in full agreement with the expected operator content of the free scalar CFT. These results strongly suggest that our model at the optimized parameter is well approximated by the tricritical Ising point with negligible corrections from the ϕ^6 interaction, i.e., the free scalar CFT.

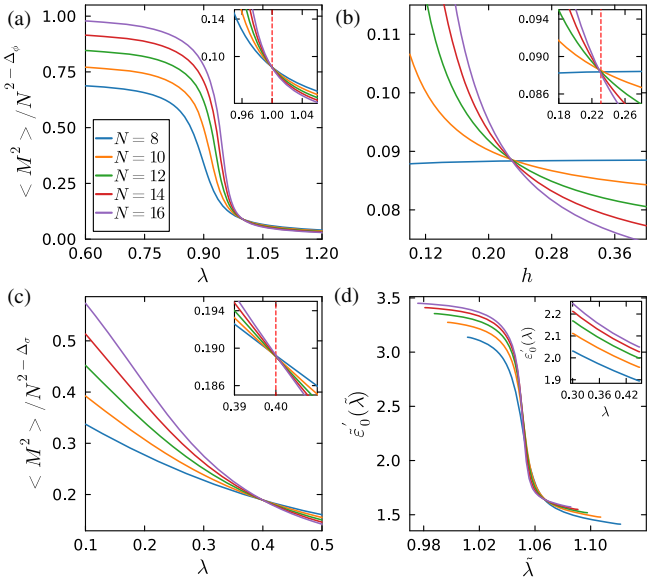

FIG. 2. Finite-size scaling across different parts of the phase diagram. (a) Scaled magnetization, $\langle M^2 \rangle / N^{2-\Delta_\phi}$ with $\Delta_\phi = 1/2$, as λ is varied through the tricritical point at fixed $h = 0.23$. The inset magnifies the crossing around $\lambda = 1$. (b) Same as (a) but fixing $\lambda = 1$ and varying h. (c) Similar to (a) but crossing the 3D Ising line at a fixed $h = 2$ by varying λ and rescaling via $\Delta_\sigma = 0.518\,148\,9$. (d) The derivative of the ground state energy density ε_0' with respect to λ at fixed $h = 0.05$. The curves have been shifted by $\tilde{\lambda} = \lambda + 0.57/N$ and $\tilde{\varepsilon}_0(\tilde{\lambda}) = \varepsilon_0(\tilde{\lambda}) + 5.8/N$ [33]. The developing discontinuity is in sharp contrast with the smooth behavior of the (nonrescaled) ε_0' across the Ising transition at $\lambda \approx 0.4$, shown in the inset. The system sizes shown are color consistent in all the panels.

To confirm the nature of Ising and tricritical Ising transitions, in Fig. 2 we perform detailed finite-size scaling analysis of the squared magnetization $\langle M^2 \rangle$ in three ways: by taking a slice through the tricritical point along either horizontal (λ) direction [Fig. 2(a)] or vertical (h) direction [Fig. 2(b)], and by crossing the 3D Ising line at a fixed $h = 2$ by varying λ [Fig. 2(c)]. In the first two cases, we rescale the data using $1/N^{2-\Delta_\phi}$, with $\Delta_\phi = 1/2$ corresponding to the Gaussian universality class, as logarithmic corrections are typically negligible at the system sizes accessible in numerics. In the last case we use the conformal bootstrap value Δ_σ for the 3D Ising [3]. We observe a clear crossing in Figs. 2(a) and 2(b), consistent with $(\lambda, h) \approx (1, 0.23)$ being a tricritical point. Similarly, the data in Fig. 2(c) are in agreement with 3D Ising universality class along the black dashed line in Fig. 1(a).

To diagnose the first-order transition, we fix h and examine the behavior of the first derivative of the ground state energy density $\varepsilon_0 = E_0/N$ with respect to λ, Fig. 2(d). The discontinuity in ε_0' at the critical point is in sharp contrast with the smooth behavior across the Ising

transition line shown in the inset of Fig. 2(d), pointing to a clear change in behavior around the tricritical point. This is also witnessed by the behavior of second derivative $\varepsilon_0''(\lambda)$, see SM [33].

Free-boson algebra—Further evidence for the free scalar theory comes from the realization of the free boson algebra. In canonical quantization, the free scalar field ϕ on a sphere of radius R has the following mode expansion [33]:

$$\phi(\mathbf{\Omega}) = \frac{1}{\sqrt{R}} \sum_{\ell,m} \frac{1}{\sqrt{2\ell+1}} (Y_{\ell,m}(\mathbf{\Omega}) \phi_{\ell,m} + \text{H.c.}), \quad (2)$$

where $Y_{\ell,m}(\mathbf{\Omega})$ are the spherical harmonics, $\phi_{\ell,m}$ are annihilation operators corresponding to bosonic modes with angular momentum (ℓ, m) that satisfy $[\phi_{\ell,m}, \phi^\dagger_{\ell',m'}] = \delta_{\ell,\ell'}\delta_{m,m'}$. The full Hilbert space of the free scalar can thus be constructed as a Fock space of these modes. For instance, the scalar primaries $|\phi^n\rangle$ correspond to states with n bosons in the $\ell = 0$ mode. To probe this Fock space structure, we can study how pseudospin operators encode the boson creation and annihilation operators. Let us write the total pseudospin operator $N_z = \int (n_\uparrow(\mathbf{\Omega}) - n_\downarrow(\mathbf{\Omega})) d^2\mathbf{\Omega}$ via the boson operators in the following symmetry-allowed form:

$$\tilde{N}_z = \frac{N_z}{(\sqrt{N})^{2-\Delta_\phi}} = a_1 \phi_{0,0} + \frac{a_3}{\sqrt{N}} \phi^3_{0,0} + \text{h.c.} + \cdots, \quad (3)$$

where ellipsis are higher order terms, and we introduced a rescaling factor so that a_1, a_3 do not depend on the system size. In a strict free scalar CFT, matrix elements of N_z between Fock states satisfy

$$p(n) = \langle \phi^n | \tilde{N}^n_z | 0 \rangle = \sqrt{n!} a_1^n + \mathcal{O}(R^{-1}), \quad (4)$$

where the subleading corrections account for mixing with higher-order terms like ϕ_0^3.

We numerically computed $p(n)$ and plot the result for $p(n)/\sqrt{n!}$ in Fig. 3. At a finite size, deviations do appear at large n. After a finite-size scaling using Eq. (4), we obtain the values shown as crosses in Fig. 3(a), which fall on a straight line—consistent with the prediction. By contrast, repeating the same calculation at a 3D Ising point, one can see a clear breakdown of Eq. (4) [33]. Similarly, the $\mathbb{Z}_2$-even total pseudospin operator takes the form $N_x = a_0 + a_2 \sum_{\ell,m} \phi^\dagger_{\ell,m} \phi_{\ell,m} + \cdots$, which can be used to measure the boson number in each energy eigenstate. As shown in SM [33], the measured expectation values in each eigenstate are indeed close to integers. This not only provides evidence for the realization of the free boson algebra, but also offers a practical diagnostic to distinguish certain primary states from descendants.

Conformal perturbations—More rigorously, the system at the optimized parameter is a free scalar theory perturbed

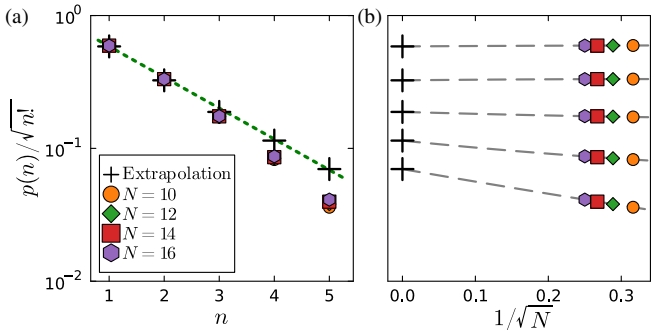

FIG. 3. Emergence of the free-boson algebra at the tricritical point. (a) $p(n)/\sqrt{n!}$ for different system sizes. The extrapolated values (crosses) follow a linear dependence with n on a log scale (dashed line), consistent with Eq. (4). (b) The extrapolated values shown in panel (a), obtained up to quadratic order in $1/\sqrt{N}$.

by small but finite interactions. We can quantitatively characterize it by the following effective description of the microscopic Hamiltonian [18,39]

$$H = \frac{v}{R} H_{\text{CFT}} + \int (g_2 \phi^2(\mathbf{\Omega}) + g_4 \phi^4(\mathbf{\Omega}) + g_6 \phi^6(\mathbf{\Omega})) d^2\mathbf{\Omega}, \quad (5)$$

where H_{CFT} is the free scalar CFT Hamiltonian, v is a nonuniversal speed of light, and irrelevant perturbations are ignored. While the numerically obtained spectrum exhibits slight deviations from the exact CFT predictions, these discrepancies are well accounted for at linear order using Eq. (5). Figure 4(a) shows the extracted effective couplings of the relevant terms are generally nonzero but sufficiently small, rendering the free scalar CFT an accurate description

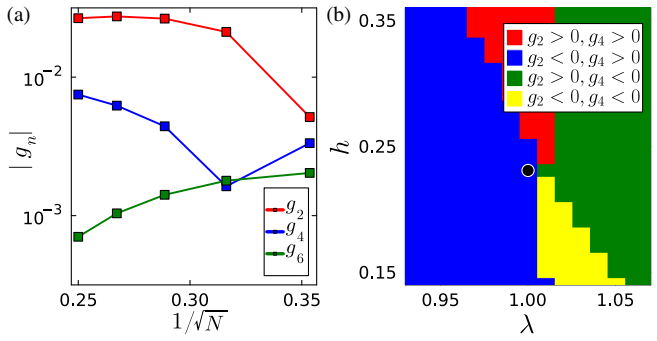

FIG. 4. Effective couplings near the tricritical point. We determine the effective coupling using six excited states that correspond to $\phi, \phi^2, \phi^3, \phi^4$ and $\partial\phi, \partial\phi^2$. The normalization is chosen such that the matrix elements of the operators ϕ^{2n} are independent of system size. (a) $g_2 < 0$, $g_6 > 0$ across all the system sizes, $g_4 < 0$ at $N = 8$ and $g_4 > 0$ for $N > 8$. (b) $g_6 > 0$ near the back dot and $g_6 < 0$ deeper inside the ferromagnetic phase (bulk of the blue region).

for moderate system sizes ($N \leqslant 16$). In larger systems, we observe that the energy gap vanishes linearly with $1/\sqrt{N}$, and the two-point function continues to display the expected algebraic decay at long distances, as confirmed by density matrix renormalization group calculation up to $N = 54$ [33]. These results suggest that the relevant couplings may remain negligible in the thermodynamic limit and the system at the optimized parameter still flows toward the free scalar.

We also apply Eq. (5) in the vicinity of the optimized parameter, Fig. 4(b). The optimized point lies near the intersection where both g_2 and g_4 change sign. The second-order Ising transition line aligns closely with the region where $g_4 > 0$ and g_2 changes sign, and the first-order transition line lies within the yellow regime, close to the boundary where g_2 changes sign. This motivates a comparison between the phase diagram from our nonperturbative analysis in Fig. 2 and one obtained by treating Eq. (5) within Ginzburg-Landau theory [40] using these couplings. The later is a mean-field calculation based on an assumption that the effective couplings in the thermodynamic limit coincide with those extracted on the finite-size sphere in Fig. 4(b). The alignment of the optimized point and transition lines indicates broad consistency between the two—further evidence for the small finite-size effects and weak coupling nature of our theory. The small discrepancies may come from the assumptions of the second calculation or residual finite-size effect. A more interesting possibility, especially for the first-order transition, is that the discrepancy comes from the positive coupling between ϕ^2 and the background curvature [18]—a new feature in the fuzzy-sphere-regularized QFT, which we reserve for future study.

Conclusions—In this Letter, we used Ising tricriticality to realize the free scalar CFT on the fuzzy sphere. The access to a free theory provides the minimal setting for understanding several aspects of the fuzzy sphere regularization. While CFTs are characterized by the conformal algebra, charge-neutral excitations in the LLL are governed by the Girvin-MacDonald-Platzman (GMP) algebra [41]. It is therefore natural to ask how the GMP algebra, when projected onto the low-energy subspace, encodes the conformal algebra [42,43]. Another question is how to extract all universal CFT data only from the LLL since the higher Landau levels are conceptually part of the ultraviolet degrees of freedom within the fuzzy sphere regularization scheme. For example, the free theory might have an efficient variational wave function description that would allow us to understand the universal data in the orbital-cut entanglement and better extract the F function [11,44]. Finally, an obvious next step is to explore how to realize the free fermion CFT, which, together with the current result, could provide a proof of principle that the fuzzy sphere regularization can potentially encompass all renormalizable QFTs.

Computational portions of this research have made use of DiagHam [45] and FuzzifiED [46] software libraries.

Note added—Recently, we became aware of a related work [47], which directly approaches the free scalar by drawing insights from its Euclidean action.

Acknowledgments—We thank Ehud Altman, Zhehao Dai, Andrew Hallam, Yin-Chen He, Chong Wang, and Michael Zaletel for helpful discussion. Computational portions of this research were carried out on ARC4 and AIRE, part of the High-Performance Computing facilities at the University of Leeds. J. T., C. V., and Z. P. acknowledge support by the Leverhulme Trust Research Leadership Award No. RL-2019-015 and EPSRC Grants No. EP/Z533634/1, No. UKRI1337. R. F. is supported by the Gordon and Betty Moore Foundation (Grant No. GBMF8688). This research was supported in part by grant NSF PHY-2309135 to the Kavli Institute for Theoretical Physics (KITP). Z. P. acknowledges support by the Erwin Schrödinger International Institute for Mathematics and Physics.

Data availability—The data that support the findings of this article are openly available [48].

[1] S. Rychkov, *EPFL Lectures on Conformal Field Theory in D >= 3 Dimensions*, SpringerBriefs in Physics (Springer, Cham, 2016).
[2] D. Simmons-Duffin, The conformal bootstrap, in *Theoretical Advanced Study Institute in Elementary Particle Physics: New Frontiers in Fields and Strings* (World Scientific, Singapore, 2017), pp. 1–74.
[3] D. Poland, S. Rychkov, and A. Vichi, The conformal bootstrap: Theory, numerical techniques, and applications, Rev. Mod. Phys. **91**, 015002 (2019).
[4] J. L. Cardy, Conformal invariance and universality in finite-size scaling, J. Phys. A **17**, L385 (1984).
[5] *The Quantum Hall Effect*, edited by R. E. Prange and S. M. Girvin (Springer-Verlag, New York, 1987).
[6] W. Zhu, C. Han, E. Huffman, J. S. Hofmann, and Y.-C. He, Uncovering conformal symmetry in the 3D Ising transition: State-operator correspondence from a quantum fuzzy sphere regularization, Phys. Rev. X **13**, 021009 (2023).
[7] L. Hu, Y.-C. He, and W. Zhu, Operator product expansion coefficients of the 3D Ising criticality via quantum fuzzy spheres, Phys. Rev. Lett. **131**, 031601 (2023).
[8] C. Han, L. Hu, W. Zhu, and Y.-C. He, Conformal four-point correlators of the three-dimensional Ising transition via the quantum fuzzy sphere, Phys. Rev. B **108**, 235123 (2023).
[9] G. Fardelli, A. L. Fitzpatrick, and E. Katz, Constructing the infrared conformal generators on the fuzzy sphere, SciPost Phys. **18**, 086 (2025).
[10] R. Fan, Note on explicit construction of conformal generators on the fuzzy sphere, arXiv:2409.08257.

[11] L. Hu, W. Zhu, and Y.-C. He, Entropic F function of three-dimensional Ising conformal field theory via fuzzy sphere regularization, Phys. Rev. B **111**, 155151 (2025).

[12] L. Hu, Y.-C. He, and W. Zhu, Solving conformal defects in 3D conformal field theory using fuzzy sphere regularization, Nat. Commun. **15**, 3659 (2024).

[13] Z. Zhou, D. Gaiotto, Y.-C. He, and Y. Zou, The g-function and defect changing operators from wavefunction overlap on a fuzzy sphere, SciPost Phys. **17**, 021 (2024).

[14] Z. Zhou and Y. Zou, Studying the 3D Ising surface CFTs on the fuzzy sphere, SciPost Phys. **18**, 031 (2025).

[15] M. Dedushenko, Ising BCFT from fuzzy hemisphere, arXiv:2407.15948.

[16] C. Han, L. Hu, and W. Zhu, Conformal operator content of the Wilson-Fisher transition on fuzzy sphere bilayers, Phys. Rev. B **110**, 115113 (2024).

[17] C. Voinea, R. Fan, N. Regnault, and Z. Papić, Regularizing 3D conformal field theories via anyons on the fuzzy sphere, Phys. Rev. X **15**, 031007 (2025).

[18] A. M. Läuchli, L. Herviou, P. H. Wilhelm, and S. Rychkov, Exact diagonalization, matrix product states and conformal perturbation theory study of a 3D Ising fuzzy sphere model, SciPost Phys. **19**, 076 (2025).

[19] M. Ippoliti, Roger S. K. Mong, F. F. Assaad, and M. P. Zaletel, Half-filled Landau levels: A continuum and sign-free regularization for three-dimensional quantum critical points, Phys. Rev. B **98**, 235108 (2018).

[20] Z. Zhou, L. Hu, W. Zhu, and Y.-C. He, SO(5) deconfined phase transition under the fuzzy-sphere microscope: Approximate conformal symmetry, pseudo-criticality, and operator spectrum, Phys. Rev. X **14**, 021044 (2024).

[21] B.-B. Chen, X. Zhang, Y. Wang, K. Sun, and Z. Y. Meng, Phases of $(2+1)$D SO(5) nonlinear sigma model with a topological term on a sphere: Multicritical point and disorder phase, Phys. Rev. Lett. **132**, 246503 (2024).

[22] B.-B. Chen, X. Zhang, and Z. Y. Meng, Emergent conformal symmetry at the multicritical point of $(2+1)$D SO(5) model with Wess-Zumino-Witten term on a sphere, Phys. Rev. B **110**, 125153 (2024).

[23] S. Yang, Y.-G. Yue, Y. Tang, C. Han, W. Zhu, and Y. Chen, Microscopic study of 3D Potts phase transition via fuzzy sphere regularization, Phys. Rev. B **112**, 024436 (2025).

[24] R. Fan, J. Dong, and A. Vishwanath, Simulating the non-unitary Yang-Lee conformal field theory on the fuzzy sphere, arXiv:2505.06342.

[25] E. A. Cruz, I. R. Klebanov, G. Tarnopolsky, and Y. Xin, Yang-Lee quantum criticality in various dimensions, arXiv:2505.06369.

[26] J. E. Miro and O. Delouche, Flowing from the Ising model on the fuzzy sphere to the 3D Lee-Yang CFT, J. High Energy Phys. 10 (2025) 037.

[27] Z. Zhou and Y.-C. He, 3D conformal field theories with Sp(N) global symmetry on a fuzzy sphere, Phys. Rev. Lett. **135**, 026504 (2025).

[28] J. Cardy, *Scaling and Renormalization in Statistical Physics* (Cambridge University Press, Cambridge, England, 1996), Vol. 5.

[29] J. Henriksson, The tricritical Ising CFT and conformal bootstrap, J. High Energy Phys. 08 (2025) 031.

[30] M. Blume, Theory of the first-order magnetic phase change in UO_2, Phys. Rev. **141**, 517 (1966).

[31] H. Capel, On the possibility of first-order phase transitions in Ising systems of triplet ions with zero-field splitting, Physica (Utrecht) **32**, 966 (1966).

[32] F. D. M. Haldane, Fractional quantization of the Hall effect: A hierarchy of incompressible quantum fluid states, Phys. Rev. Lett. **51**, 605 (1983).

[33] See Supplemental Material at http://link.aps.org/supplemental/10.1103/cj3l-cf58 for details of the derivations and further numerical results.

[34] T. Grover, D. N. Sheng, and A. Vishwanath, Emergent space-time supersymmetry at the boundary of a topological phase, Science **344**, 280 (2014).

[35] A. Rahmani, X. Zhu, M. Franz, and I. Affleck, Emergent supersymmetry from strongly interacting Majorana zero modes, Phys. Rev. Lett. **115**, 166401 (2015).

[36] E. O'Brien and P. Fendley, Lattice supersymmetry and order-disorder coexistence in the tricritical Ising model, Phys. Rev. Lett. **120**, 206403 (2018).

[37] K. Moon, H. Mori, K. Yang, S. M. Girvin, A. H. MacDonald, L. Zheng, D. Yoshioka, and S.-C. Zhang, Spontaneous interlayer coherence in double-layer quantum Hall systems: Charged vortices and Kosterlitz-Thouless phase transitions, Phys. Rev. B **51**, 5138 (1995).

[38] B. I. Halperin, P. A. Lee, and N. Read, Theory of the half-filled Landau level, Phys. Rev. B **47**, 7312 (1993).

[39] B.-X. Lao and S. Rychkov, 3D Ising CFT and exact diagonalization on icosahedron: The power of conformal perturbation theory, SciPost Phys. **15**, 243 (2023).

[40] P. M. Chaikin, T. C. Lubensky, and T. A. Witten, *Principles of Condensed Matter Physics* (Cambridge University Press, Cambridge, England, 1995), Vol. 10.

[41] S. M. Girvin, A. H. MacDonald, and P. M. Platzman, Magneto-roton theory of collective excitations in the fractional quantum Hall effect, Phys. Rev. B **33**, 2481 (1986).

[42] A. Cappelli, C. A. Trugenberger, and G. R. Zemba, Infinite symmetry in the quantum Hall effect, Nucl. Phys. **B396**, 465 (1993).

[43] A. Gromov and D. T. Son, Bimetric theory of fractional quantum Hall states, Phys. Rev. X **7**, 041032 (2017).

[44] H. Li and F. D. M. Haldane, Entanglement spectrum as a generalization of entanglement entropy: Identification of topological order in non-Abelian fractional quantum Hall effect states, Phys. Rev. Lett. **101**, 010504 (2008).

[45] DiagHam, https://www.nick-ux.org/diagham.

[46] Z. Zhou, FuzzifiED—Julia package for numerics on the fuzzy sphere, arXiv:2503.00100.

[47] Y.-C. He, Free real scalar CFT on fuzzy sphere: Spectrum, algebra and wavefunction ansatz, arXiv:2506.14904.

[48] J. Taylor, C. Voinea, Z. Papić, and R. Fan, 10.5518/1789.